



## Synthesis of surface imprinted polymer upon modified kaolinite and study on the selective adsorption of BPA

Yanli Mao<sup>a,b,\*</sup>, Haiyan Kang<sup>a</sup>, Yifei Guo<sup>a</sup>, Songtao Chen<sup>a</sup>, Zengxin Wang<sup>a</sup>

<sup>a</sup>*School of Municipal and Environmental Engineering, Henan University of Urban Construction, Pingdingshan 467000, China, Tel. +86 13721877188; email: myanliao@163.com (Y. Mao), Tel. +86 15937595806; email: kanghaiyan@hncj.edu.cn (H. Kang), Tel. +86 13603755706; email: gyifei@hncj.edu.cn (Y. Guo), Tel. +86 18537505879; email: cst@hncj.edu.cn (S. Chen), Tel. +86 13083757777; email: wzx@hncj.edu.cn.com (Z. Wang)*

<sup>b</sup>*School of Chemistry and Chemical Engineering, Jiangsu University, Zhenjiang 212013, China*

Received 11 April 2014; Accepted 11 November 2014

### ABSTRACT

Using bisphenol A (BPA) as the template and the modified kaolinite as solid-support substrates, a novel surface molecularly imprinted polymer (S-MIPs) was prepared by combining self-assembly molecular imprinting technology and sacrificial support process. The resulting composites were characterized by transmission electron microscopy, thermogravimetric analysis, and nitrogen adsorption–desorption. The results of batch adsorption experiments suggested that pH 6.0 in testing solution was the optimal adsorption condition. The kinetic properties of S-MIPs were well described by the pseudo-second-order equation, which indicated that chemical process could be the rate-limiting step in the adsorption process for BPA. Equilibrium data were described by the Langmuir and Freundlich isotherm models. Results suggested that Langmuir isotherm model was fitted to the experimental data significantly better than the other models. Selectivity experiments showed the high affinity of target BPA over competitive compounds than those of non-imprinted polymers. Moreover, the reuse of S-MIPs was affirmed in five sequential cycles of adsorption/desorption, without significant loss in adsorption capacity.

*Keywords:* Kaolinite; Bisphenol A (BPA); Surface imprinting technology; Selective adsorption

### 1. Introduction

Bisphenol A (BPA) is a high production volume chemical used in a variety of applications, including epoxy resins that line food and beverage cans [1,2]; hard polycarbonate plastics such as water bottles, food storage containers, medical devices, baby toys, and thermal receipt papers and carbonless copy [3]. Besides, it is widely used in a number of products such as building materials, adhesives, and powder paints

[4]. It is well known that BPA causes not only various diseases including cancer [5,6], but also a strong estrogenic endocrine disrupting effect [7,8]. And BPA has an acute toxicity in the range  $\sim 1\text{--}10\text{ mg L}^{-1}$  [9]. Researchers have found the BPA contamination in industrial wastewater, surface waters, groundwater, and even drinking water [10]. BPA has been listed in the priority pollutants into the aquatic environment by China and the United States Environmental Protection Agency (USEPA) due to its stability, bioaccumulation, and toxicity [11,12]. In regular monitoring, selective

\*Corresponding author.

recognition, and removal of target bisphenol from complex matrixes in environment is frequently required. Thus, the great priority has been given to the development of novel molecular recognition and selective separation techniques.

Molecule imprinting is a powerful technique for synthesizing molecularly imprinted polymers (MIPs) with specific molecular recognition properties [13]. Owing to the mechanical, chemical, and thermal stability, easy and cheap preparation together with high selectivity for the template molecules, MIPs have been applied in many fields, such as solid-phase extraction [14], drug design [15], and sensor devices [16], water treatment [17], and so on, where the MIPs act as a “artificial antibodies.” Traditionally, MIPs are prepared by the bulk copolymerization of functional monomer and cross-linker in the presence of template molecule. However, the bulk MIPs prepared by the conventional method exhibit some disadvantages such as low affinity binding, high diffusion barrier, poor site accessibility, and low-rate mass transfer [18]. Recently, the surface imprinting technique has been proposed by creating the imprinted cavities with high affinity imprinted sites on the surface of a suitable matrix, which provides an alternative way to improve mass transfer and reduce permanent entrapment of the template [19]. In previous researches, SiO<sub>2</sub> [20], Fe<sub>3</sub>O<sub>4</sub> nanoparticles [21], polystyrene core colloids [22], and carbon nanotubes [23] have been widely used in the surface imprinting process.

When compared with conventional solid-support substrates, modified kaolinite has been proved to be efficient and promising materials. The 1:1 dioctahedral layered mineral kaolinite Al<sub>2</sub>Si<sub>2</sub>O<sub>5</sub>(OH)<sub>4</sub> is one of the most ubiquitous clays on earth [24]. It has two different basal planes: Tetrahedral siloxane surface of Si–O–Si exposure and octahedral aluminum oxyhydroxyl (Al–O–OH) surface of Al–OH exposure, both of these surfaces are theoretically electrically neutral. The kaolinite lamellae are stacked in a polar mode by strong hydrogen bonds, forming platy crystals approximately 100 nm thick [25–27]. Due to its special structure and high surface area, kaolinite is easy to be modified by surfactants and silane coupling agent [28,29]. In contrast with other nanosized materials, kaolinite are readily obtainable, much cheaper. Therefore, it could be a potential solid-support material in synthesizing surface imprinting polymer for its particular intensity and stable chemical property together with low cost.

The aim of this study was to synthesize surface MIPs using BPA as a template molecule, methacrylic acid (MAA) as a functional monomer, azodiisobutyronitrile (AIBN) as initiator, and ethylene glycol dimethacrylate

(EGDMA) as a cross-linker. The results showed that S-MIPs demonstrated the higher affinity for target BPA and excellent regeneration property when compared with those of non-imprinted polymers (NIPs). The prepared S-MIPs were successfully applied to the selective solid-phase extraction and separation of BPA from environmental samples.

## 2. Experimental section

### 2.1. Reagents and instruments

Kaolinite (KLT) was collected from Zhengzhou Jinyangguang Chinaware Co. Ltd., Henan, China. EGDMA, poly(vinylpyrrolidone) (PVP), dimethyl sulfoxide (DMSO), and HPLC-grade methanol were obtained from Sinopharm Chemical Reagent Co., Ltd. (Shanghai, China). BPA, 4,4-biphenyl diphenol (4,4-BIP), 2,6-dichlorophen (2,6-DCP), and AIBN were obtained from Aladdin Reagent Co., Ltd. (Shanghai, China). Oleic acid (OA), MAA, anhydrous ethanol, methanol, acetonitrile, acetone, and hydrofluoric acid were purchased from Sinopharm Chemical Reagent Co., Ltd. (Shanghai, China). All other chemicals were supplied by local suppliers and used without further purification.

The morphology of S-MIPs was observed by transmission electron microscope (TEM, JEOL IEM-200CX). Thermogravimetric analysis (TGA) of samples was performed for powder samples (about 10 mg) using a Diamond TG/DTA instruments (Perkin–Elmer, USA) under a nitrogen atmosphere up to 800 °C with a heating rate of 5.0 °C/min. UV–Vis spectrophotometer was also used to analyze the samples. High-performance liquid chromatography equipped with a UV detector was used for the detection of BPA, 4,4-BIP, and 2,6-DCP. PHS-3c type acidity meter, Autosorb-1-c adsorption instrument, 802 centrifugal precipitator were also used in our work.

### 2.2. Experiment

#### 2.2.1. Preparation of modified kaolinite surface molecularly imprinted polymers (S-MIPs)

Preparation of modified kaolinite S-MIPs was implemented by following steps mentioned in the previous literature with a few modifications [30–32]. Typically, the 0.2283 g of BPA and 0.68 mL of MAA were added into 30 mL of DMSO in a three-necked flask. This mixture was stirred for 30 min for preparation of the preassembly solution. The 2.0 g of the modified KLT, 2.0 mL of OA, and 6.8 mL of EGDMA were mixed in flask; the preassembly solution was

also added into the flask and stirred constantly. The mixture was subjected to ultrasound for 30 min for preparation of the prepolymerization solution. The 0.4 g of PVP used as surfactants was dissolved into 150 mL of DMSO:water (V/V = 9:1) in a three-necked round-bottomed flask. The mixture was stirred and purged with nitrogen gas to displace oxygen while the temperature increased to 60°C. The prepolymerization solution was added into the three-necked flask, and then the 0.2 g of AIBN was also added into the mixture as an initiator. The reaction was allowed to proceed at 60°C for 24 h. After the polymerization, the obtained polymers were washed with the mixture solution of methanol/acetic acid (V/V = 8:2) using soxhlet extraction to remove the template molecules, until the template molecule could not be detected by UV–Vis spectrophotometer. Finally, the obtained MIPs were dried at 60°C in a vacuum oven; the dried MIPs and 50 mL of HF were poured into a Teflon plastic beaker and sealed, after stirring for 12 h, and then filtered and washed, yielding the desired S-MIPs. In comparison, NIPs without the template molecules (BPA) were prepared in parallel with the MIP using the same synthetic procedure, but synthetic products were not decomposed by HF.

### 2.2.2. The single factor effect on adsorption behavior of BPA

In batch adsorption experiments, a certain amount of adsorbent and a certain concentration of BPA solution were added into a 25 mL colorimetric cylinder, the effect of adsorbent dosage (0.005–0.15 g), solution pH (2.0–10.0), temperatures (25, 35, and 45°C), and concentration (20–500 mg L<sup>-1</sup>) were studied by batch mode experiment. After the reaction, the mixed liquid was kept for 12 h. The supernatant was got after centrifugation, and BPA concentration in the supernatant was measured by using the HPLC, the equilibrium adsorption capacity was calculated according to the formula (1)

$$Q_t = \frac{(C_0 - C_t)V}{W} \quad (1)$$

where  $C_0$  (mg L<sup>-1</sup>) and  $C_t$  (mg L<sup>-1</sup>) are the initial and at any time  $t$  concentration of BPA, respectively.  $V$  (L) and  $W$  (g) are the solution volume and the mass of adsorbent, respectively.

### 2.2.3. Competitive adsorption

From the two compounds (4,4'-BIP and 2,6-DCP), the structure which is similar to BPA was chosen. Three kinds of molecular structural formula were shown in Fig. 1. The solutions of BPA, 4,4'-BIP, and 2,6-DCP were prepared. All the concentrations were 100 mg L<sup>-1</sup>. Ten milliliter of three element mixed solution and 0.02 g of S-MIPs or NIPs were added into a 25 mL of colorimetric tube, and kept for 12 h, target and competition component concentration of the supernatant was analyzed by HPLC. The main operating conditions of HPLC were as follows: 278 nm (analytical wavelength), mixture of 65% methanol and 35% deionized water (mobile phase), and 1.0 mL min<sup>-1</sup> (flow rate).

## 3. Results and discussion

### 3.1. Characterization

#### 3.1.1. Transmission electron microscope

The morphology of MIPs and S-MIPs was observed by TEM was shown in Fig. 2(a) and (b). When compared with this two pictures, it can be clearly seen that the middle part shown in Fig. 2(a) which represented the coarser structure of the MIPs is black and it could be thought as kaolinite wrapped in the middle of MIPs layer. Interestingly, it was observed that the color of S-MIPs particles was light as shown in Fig. 2(b) when the part of kaolinite substrate material was decomposed by HF.

#### 3.1.2. BET analysis

Autosorb-1-c nitrogen adsorption instrument was used in the experiment. Typically, the sample was pre-desorption for 12 h at 150°C and measured fully by

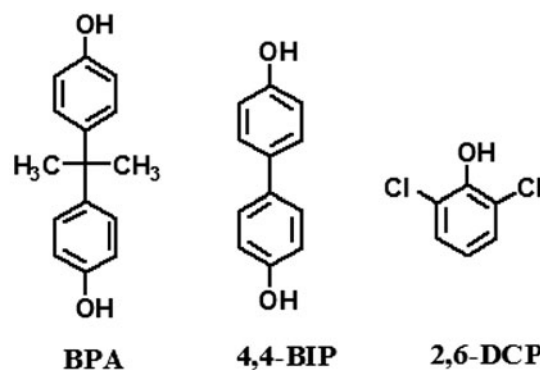


Fig. 1. Chemical structure of BPA, 4,4'-BIP and 2,6-DCP.

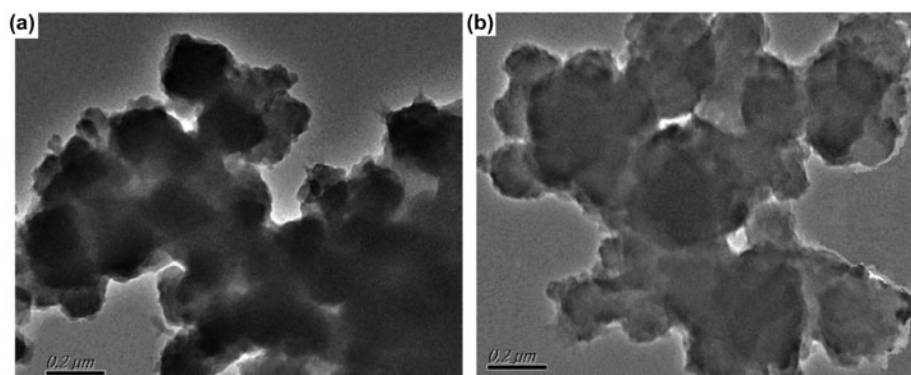


Fig. 2. TEM micrographs of (a) MIPs and S-MIPs (b).

the nitrogen adsorption/desorption method. And then the BET of the sample was calculated according to BET equation. As seen in Table 1, the difference of specific surface area, pore volume and pore size of the MIPs and NIPs was small; the larger specific surface area and pore volume of the S-MIPs was favorable for adsorption of BPA from aqueous solution.

### 3.1.3. TGA

The TGA of MIPs and S-MIPs were shown in Fig. 3. Weight loss of the MIPs and S-MIPs was assigned to the water quality between 25 and 200°C, which was 11.39 and 5.42%, respectively. For MIPs, the polymer which was wrapped on the surface kaolinite was all burnt off at the temperature of 200–800°C, the quality of remaining kaolinite was 32.42%. For S-MIPs, while the quality of remaining was only 5.58%, this should be attributed to partial kaolinite which could not be completely decomposition by HF, and the quality of the kaolinite decomposed by HF was 26.84%.

## 3.2. Adsorption experiments

### 3.2.1. Effect of adsorbent dosage

To study the effect of adsorbent dosage on the removal of BPA from aqueous solutions, the different

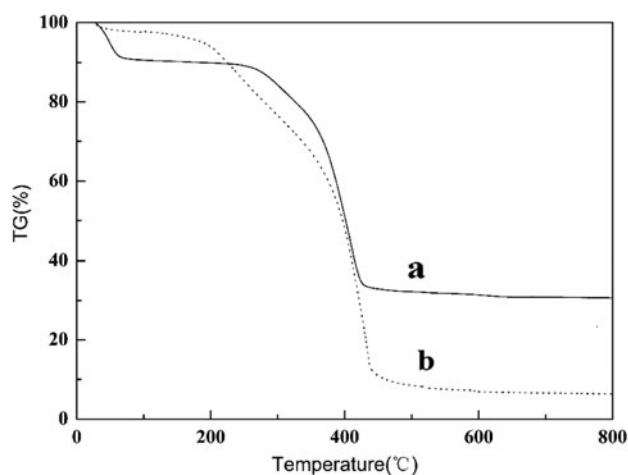


Fig. 3. TGA of modified MIPs (a) and S-MIPs (b).

dosage of the adsorbent ranging from 0.005 to 0.15 g was dispersed in 50 mL colorimetric cylinder containing 25 mL of 250 mg L<sup>-1</sup> of BPA solution (pH 6.0) at 25°C for 12 h, respectively. As seen in Fig. 4, the equilibrium adsorption capacity of BPA increased rapidly at first, and occurred a slower phase, and then declined. When the S-MIPs dosage was doubled, the equilibrium adsorption capacity of BPA increased from 123.45 to 249.26 mg g<sup>-1</sup>, which was due to the specific adsorption sites of the adsorbent and the more

Table 1  
Results of nitrogen biosorption measurements

Sample	BET (m <sup>2</sup> g <sup>-1</sup> )	Pore volume (cm <sup>3</sup> g <sup>-1</sup> )	Diameter (nm)
KLT	7.62	0.029	15.04
MIPs	142.90	0.158	4.41
NIPs	150.80	0.177	4.68
S-MIPs	340.8	0.432	8.21

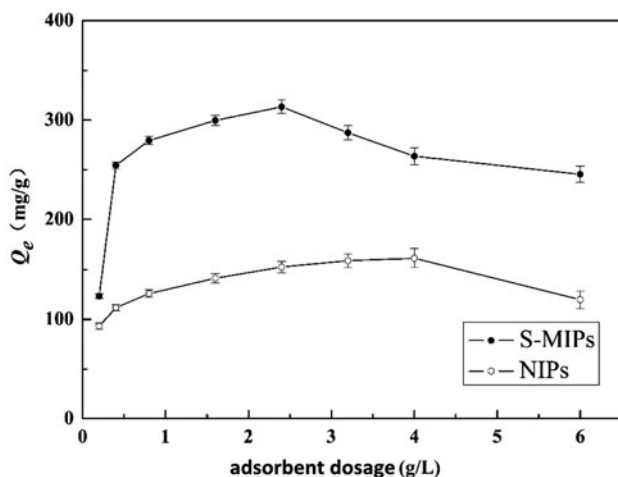


Fig. 4. Effect of adsorbent dosage.

holes of MIPs after decomposition by HF. When the adsorbent dosage increased from 1.6 to 2.4 g L<sup>-1</sup>, the corresponding equilibrium adsorption capacity increased from 279.35 to 313.23 mg g<sup>-1</sup>, the increase multiples of adsorption capacity were not consistent with the increase in adsorbent dosage, which was assigned to the target molecules in solution was not increased, causing the competition effect occurred. When adsorbent dosage increased from 3.2 to 6.0 g L<sup>-1</sup>, the unit adsorption capacity showed a decline trend, the increase in adsorbent dosage provided more adsorption sites for BPA, resulting in a lower distribution of BPA on the unit adsorbent thus, equilibrium adsorption capacity began to decline.

### 3.2.2. The effect of pH

To study the effect of pH on the removal of BPA from aqueous solutions, 0.018 g of adsorbent was dispersed in 25 mL colorimetric cylinder containing 10 mL of 100 mg L<sup>-1</sup> of BPA solution, respectively. The initial pH value of the solution was adjusted from 2.0 to 10.0 using 0.1 mol L<sup>-1</sup> HCl or NaOH solutions. The reaction was allowed to proceed at 25°C for 12 h. As illustrated in Fig. 5, the equilibrium adsorption capacity of BPA increased from 67.13 to 79.98 mg g<sup>-1</sup> with increasing pH from 2.0 to 6.0, when the pH was over 7.0 and then, decreased with increasing pH. Because the pKa of the BPA is of 10.23 [33], the ionized anions from BPA increased with increasing pH of the adsorption system, which resulted in a greater exclusion for negatively charged adsorbent. The experimental results make it clear that pH 6.0 was the optimum pH.

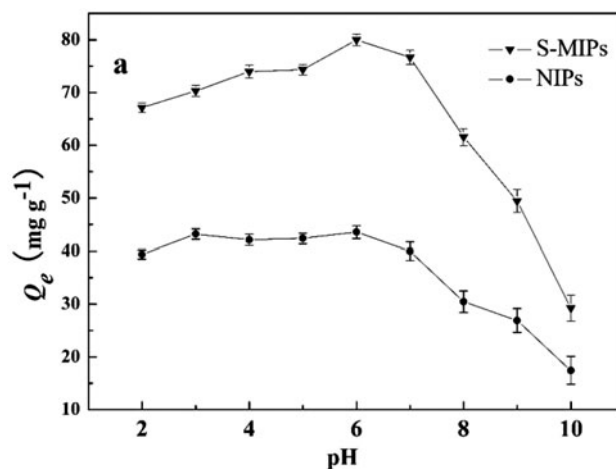


Fig. 5. Effect of initial solution pH on adsorption.

### 3.2.3. The effect of temperature

To study the effect of temperature on the removal of BPA from aqueous solutions, 0.01 g of adsorbent was dispersed in 25 mL colorimetric cylinder containing 10 mL of BPA solution (pH 6.0) of different initial concentrations 100, 150, and 200 mg L<sup>-1</sup>, respectively. The reaction was allowed to proceed for 12 h and temperature was maintained at 25, 35, and 45°C. Fig. 6 showed the effect of temperature on the adsorption of BPA by S-MIPs from solutions with different initial concentrations at different temperature. It was found that the maximum adsorption capacities of BPA were 81.45, 145.54, and 172.79 mg g<sup>-1</sup> at 25°C, respectively. While the equilibrium adsorption capacity of the BPA decreased with increase in temperature, thereby confirming that the process was exothermic.

### 3.3. Adsorption kinetics

Information on the kinetics of pollutant uptake is required for choosing optimum operating conditions for full-scale batch process. Therefore, two kinetic models including the pseudo-first-order model and pseudo-second-order model were applied to analyze the experimental data related to the adsorption of BPA onto S-MIPs and NIPs. The pseudo-first-order model and the pseudo-second-order model can be expressed as follows [34,35]:

$$\ln(Q_c - Q_t) = \ln Q_c - k_1 t \quad (2)$$

$$\frac{t}{Q_t} = \frac{1}{k_2 Q_c^2} + \frac{t}{Q_c} \quad (3)$$

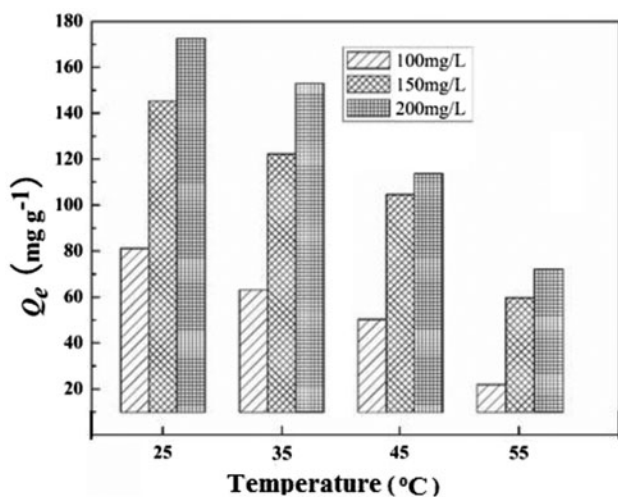


Fig. 6. Effect of temperature on adsorption of BPA onto S-MIPs.

where  $Q_e$  and  $Q_t$  are the amount of adsorbate onto adsorbent at equilibrium and at any time  $t$  ( $\text{mg g}^{-1}$ ), respectively, and  $k_1$  ( $\text{min}^{-1}$ ) and  $k_2$  ( $\text{g mg}^{-1} \text{min}^{-1}$ ) are the rate constants of pseudo-first-order model and pseudo-second-order model, respectively.

As seen in Fig. 7, the BPA adsorption on adsorbent occurred in two steps, an initial fast step which lasted for about 60 min followed by a slower second step which continued until the end of experimental period. The rapid step is probably due to the abundant availability of adsorption sites on the adsorbent. It was possible that the initial concentration of BPA molecules provided the necessary driving force to overcome the resistances of mass transfer between the aqueous phases and the solid phase.

The BPA adsorption kinetic constants and correlation coefficients were fitted by using pseudo-first-order and pseudo-second-order model, it was found that the adsorption kinetics data of BPA adsorption onto S-MIPs and NIPs fitted very well to a pseudo-second-order model. The values of correlation coefficients for the pseudo second-order kinetic model were found to be 0.9994 and 0.9989, respectively. And it was assumed that the chemical process could be the rate-limiting step in the adsorption process for BPA. As shown in Fig. 7, the equilibrium adsorption capacity for adsorption of BPA on S-MIPs was obviously higher than that of NIPs, which could be attributed to the specific adsorption sites of the MIPs and the more holes of MIPs after being decomposed by HF. Moreover, the adsorption of BPA on S-MIPs and NIPs reached saturation within 180 and 240 min, respectively.

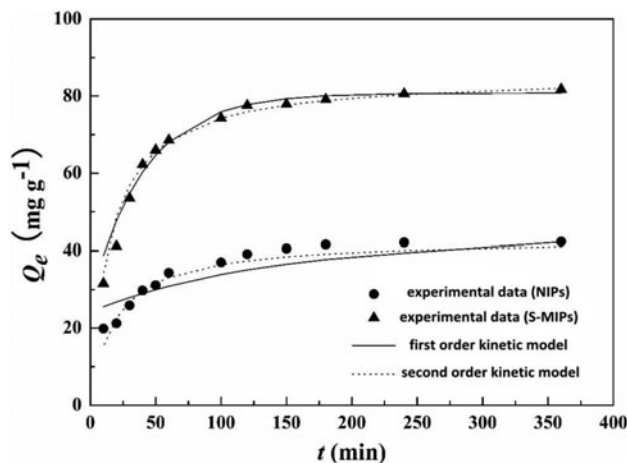


Fig. 7. Kinetic models of BPA adsorption onto S-MIPs and NIPs.

### 3.4. Adsorption isotherm

The data of adsorption equilibrium were fitted to Langmuir and Freundlich isotherms in this work. The linear Langmuir isotherm and Freundlich isotherm can be expressed as follows (4) and (5) [36,37], respectively.

$$\frac{C_e}{Q_e} = \frac{1}{Q_m K_L} + \frac{C_e}{Q_m} \quad (4)$$

$$\ln Q_e = 1/n(\ln C_e) + \ln K_f \quad (5)$$

where  $Q_e$  is the amount of BPA uptake ( $\text{mg g}^{-1}$ ) at equilibrium,  $C_e$  is the equilibrium concentration of adsorbate ( $\text{mg L}^{-1}$ ),  $Q_m$  is the maximum adsorption capacity of the adsorbent ( $\text{mg g}^{-1}$ ), and  $K_L$  is the Langmuir equilibrium constant ( $\text{L mg}^{-1}$ ) and is related to the free energy of adsorption.  $K_f$  and  $n$  are the Freundlich constants related to adsorption capacity and energy of adsorption, respectively.

The adsorption isotherms of S-MIPs and NIPs for BPA obtained at the temperatures of  $25^{\circ}\text{C}$  were given in Fig. 8. As shown in Fig. 8, when the equilibrium concentration increased, the equilibrium adsorption capacity for BPA first increased sharply, and then gradually reached saturation, and finally reached to the maximum point. Furthermore, the BPA adsorbed on S-MIPs was much higher than that of NIPs, indicating the significantly preferential adsorption of BPA for S-MIPs. It was probably because S-MIPs illustrated the good specificity for the imprinted molecule. By fitting the experimental data with Langmuir and Freundlich isotherm model, it was also found that the Langmuir isotherm model fitted

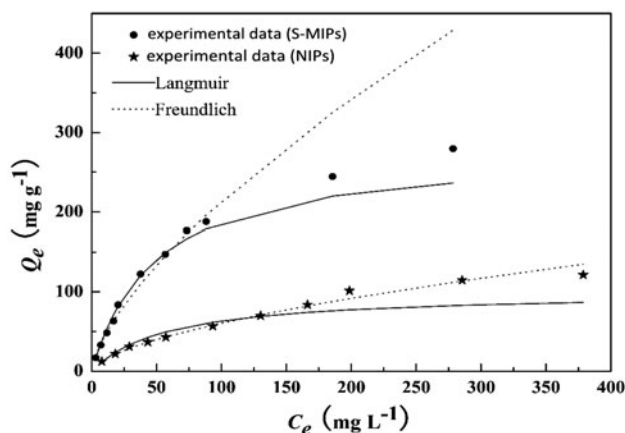


Fig. 8. Isotherms of BPA adsorption onto S-MIPs and NIPs.

the equilibrium data significantly better than the Freundlich model, the value of correlation coefficients was 0.9984, indicating monolayer molecular adsorption for S-MIPs. While the adsorption isotherm of BPA onto NIPs was better described by the Freundlich model, the correlation coefficient was 0.9967, indicating monolayer molecular adsorption for S-MIPs and multi-molecular layers adsorption for NIPs.

### 3.5. Selectivity studies of S-MIPs toward BPA

The selectivity adsorption of BPA on S-MIPs was examined by competition adsorption. The supernatant liquid chromatography of the ternary standard mixture and the standard mixture adsorbed by NIPs and S-MIPs were shown in Fig. 9(a)–(c), respectively.

The static distribution coefficient  $K_d$ , the selectivity coefficients  $k$  and relative selectivity coefficient  $k'$  were used to evaluate the selectivity of S-MIPs [38]. These parameters were calculated according to the following formula:

$$K_d = \frac{C_p}{C_s} \quad (6)$$

$$k = \frac{K_{d1}}{K_{d2}} \quad (7)$$

$$k' = \frac{k_{\text{MIP}}}{k_{\text{NIP}}} \quad (8)$$

where  $C_p$  is the adsorption concentration,  $C_s$  is the supernatant concentration.  $K_{d1}$  and  $K_{d2}$  are the static distribution coefficient of BPA and competition BPA.  $K_{\text{S-MIP}}$  and  $K_{\text{NIP}}$  represent the separation factor of S-MIPs and NIPs. The values of  $k'$  indicated adsorption

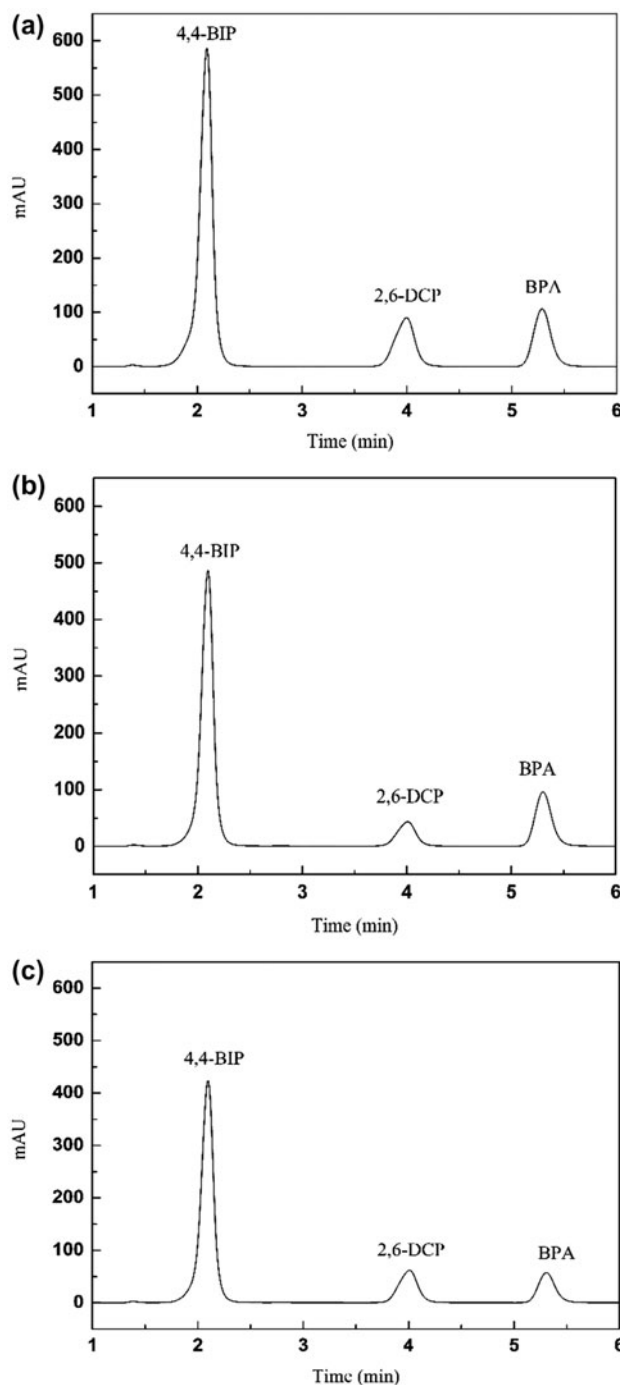


Fig. 9. Chromatograms obtained from selective adsorption. The supernatant liquid chromatogram of the ternary standard mixture (a), the standard mixture adsorbed by NIPs (b), and the standard mixture adsorbed S-MIPs (c).

selectivity and affinity of NIPs for BPA compared with S-MIPs. As seen from Fig. 9 and Table 2, the results clearly revealed that S-MIPs had high recognition selectivity and binding affinity for the template BPA.

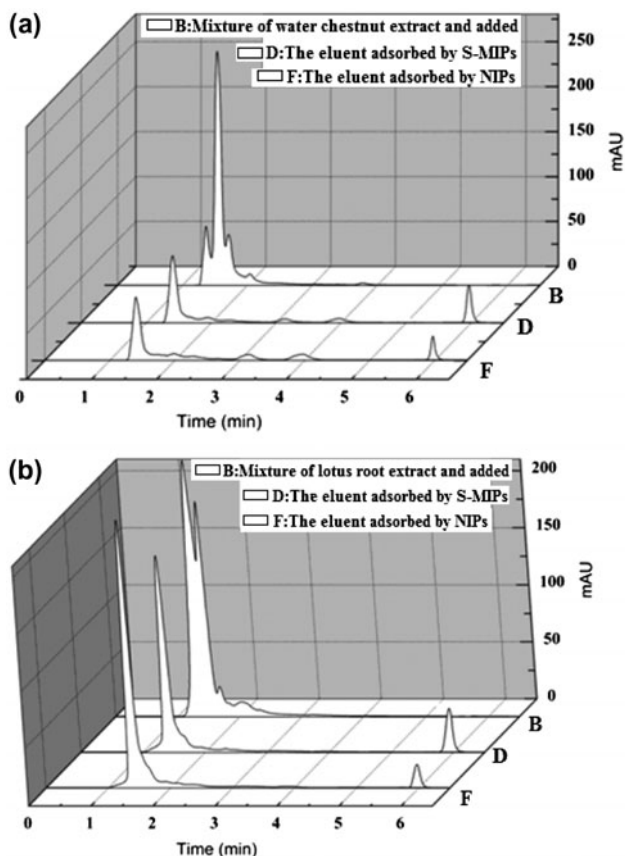


Fig. 10. HPLC chromatograms of chestnut and lotus with S-MIPs or NIPs as adsorbent. HPLC chromatograms of water chestnut extract (a) and lotus root extract (b) with S-MIPs or NIPs as adsorbent.

### 3.6. Regeneration experiment

To test the regeneration of the S-MIPs, desorption of BPA from the S-MIPs was investigated with an eluant of methanol/acetic acid (V:V = 8:2). After the supernatant solution was discarded, the S-MIPs were washed with eluant under ultrasonic bath for 30 min. After five cycles of regeneration, the equilibrium adsorption capacity of BPA slightly decreased with increasing the using times, yet the last equilibrium adsorption capacity was  $62.95 \text{ mg g}^{-1}$ , which was 77.39% of the first

adsorption capacity. It could be concluded that S-MIPs had a good regeneration performance.

### 3.7. Analysis of real samples

The aquatic plants chestnut and lotus root were chosen as analysis samples in the experiment. Mixture of the extract, spiked-treated and added solution was enriched by S-MIPs and NIPs, the eluent was determined using high-performance liquid chromatography with ultraviolet detector (HPLC-UVD), and compared with the original standard solution to evaluate the feasibility.

As seen in Fig. 10(a) and (b), the peaks of water chestnut and lotus appeared in the layer B, respectively. The eluent adsorbed by S-MIPs, the obvious characteristic peak of BPA appeared in the layer D, retention time is 5.976 and 5.884 min, respectively. Moreover, the peaks of water chestnut and lotus all decrease to a certain extent. The eluent adsorbed by NIPs, the characteristic peak of BPA appeared in the layer F, but which was slightly decreased when compared with layer D. The results indicated that of the S-MIPs showed a selective recognition ability for BPA, while the nonspecific binding sites decreased the recognition effect of the NIPs. Therefore, S-MIPs could be suitable in the sample preparation for trace analysis of BPA from complicated vegetable and water samples.

## 4. Conclusions

In this work, a novel S-MIPs was prepared by combining self-assembly molecular imprinting technology and sacrificial support process. The prepared S-MIPs were successfully applied to the selective solid-phase extraction of BPA from environmental samples. The results of batch adsorption experiments suggested that pH 6.0 in testing solution was the optimal adsorption condition. The kinetic properties of S-MIPs were well described by the pseudo-second-order equation, indicating chemical process could be the rate-limiting step in the adsorption process for BPA. Equilibrium experiments were described by the Langmuir and Freundlich isotherm models. The Langmuir isotherm model was well fitted to the equilibrium data of the S-MIPs, and the monolayer adsorption capacity of the S-MIPs was much higher than that of the NIPs. The selective recognition experiments demonstrated high affinity and selectivity toward target BPA over competitive compounds than that of NIPs. Therefore, the analytical method based on S-MIPs extraction coupled with HPLC was successfully used for BPA analysis in spiked vegetable and water samples.

Table 2  
Distribution coefficient and selectivity coefficient data

Analyte	$K_d$		$k$		$k'$
	S-MIPs	NIPs	S-MIPs	NIPs	
BPA	1.51	0.45			
4,4-BIP	0.47	0.53	3.20	0.84	3.81
2,6-DCP	0.18	0.92	8.32	0.48	17.33

## Acknowledgments

This work was financially supported by the National Natural Science Foundation of China (No. 21107037), by the Natural Science Foundation of He'nan Province (No. 2012HASTTT026), by the China Youth Foundation Postdoctoral (No. 2011M500870) and the Youth Backbone Foundation of He'nan Province (No. 2011GGJS-167).

## References

- [1] R.R. Gerona, T.J. Woodruff, C.A. Dickenson, J. Pan, J.M. Schwartz, S. Sen, M.W. Friesen, V.Y. Fujimoto, P.A. Hunt, Bisphenol-A (BPA), BPA glucuronide, and BPA sulfate in midgestation umbilical cord serum in a Northern and Central California population, *Environ. Sci. Technol.* 47 (2013) 12477–12485.
- [2] G. Mezohegyi, B. Erjavec, R. Kaplan, A. Pintar, Removal of bisphenol A and its oxidation products from aqueous solutions by sequential catalytic wet air oxidation and biodegradation, *Ind. Eng. Chem. Res.* 52 (2013) 9301–9307.
- [3] K. Lin, W.P. Liu, J. Gan, Oxidative removal of bisphenol A by manganese dioxide: Efficacy, products, and pathways, *Environ. Sci. Technol.* 43 (2009) 3860–3864.
- [4] Q. Sun, Y. Li, P. Chou, P. Peng, C. Yu, Transformation of bisphenol A and alkylphenols by ammonia-oxidizing bacteria through nitration, *Environ. Sci. Technol.* 46 (2012) 4442–4448.
- [5] T. Suzuki, Y. Nakagawa, I. Takano, K. Yaguchi, K. Yasuda, Environmental fate of bisphenol A and its biological metabolites in river water and their xenoestrogenic activity, *Environ. Sci. Technol.* 38 (2004) 2389–2396.
- [6] B. Gözmen, M.A. Oturan, N. Oturan, O. Erbatur, Indirect electrochemical treatment of bisphenol A in water via electrochemically generated Fenton's reagent, *Environ. Sci. Technol.* 37 (2003) 3716–3723.
- [7] R.A. Torres, C. Pétrier, E. Combet, F. Moulet, C. Pulgarin, Bisphenol A mineralization by integrated ultrasound-UV-iron (II) treatment, *Environ. Sci. Technol.* 41 (2007) 297–302.
- [8] W.Y. Huang, M. Brigante, F. Wu, C. Mousty, K. Hanna, G. Mailhot, Assessment of the Fe(III)-EDDS complex in Fenton-like processes: From the radical formation to the degradation of bisphenol A, *Environ. Sci. Technol.* 47 (2013) 1952–1959.
- [9] C.S. Guo, M. Ge, L. Liu, G.D. Gao, Y.C. Feng, Y.Q. Wang, Directed synthesis of mesoporous TiO<sub>2</sub> microspheres: Catalysts and their photocatalysis for bisphenol A degradation, *Environ. Sci. Technol.* 44 (2010) 419–425.
- [10] J. Xu, L. Wang, Y.F. Zhu, Decontamination of bisphenol A from aqueous solution by graphene adsorption, *Langmuir* 28 (2012) 8418–8425.
- [11] A. Schecter, N. Malik, D. Haffner, S. Smith, T. Harris, O. Paepke, L. Birnbaum, Bisphenol A (BPA) in U.S. food, *Environ. Sci. Technol.* 44 (2010) 9425–9430.
- [12] S. Fukahori, H. Ichiura, T. Kitaoka, H. Tanaka, Photocatalytic decomposition of bisphenol A in water using composite TiO<sub>2</sub>-zeolite sheets prepared by a papermaking technique, *Environ. Sci. Technol.* 37 (2003) 1048–1051.
- [13] J. Luo, S.S. Jiang, X.Y. Liu, Efficient one-pot synthesis of mussel-inspired molecularly imprinted polymer coated graphene for protein-specific recognition and fast separation, *J. Phys. Chem. C* 117 (2013) 18448–18456.
- [14] W.M. Yang, W. Zhou, W.Z. Xu, H. Li, W.H. Huang, B. Jiang, Z.P. Zhou, Y.S. Yan, Synthesis and characterization of a surface molecular imprinted polymer as a new adsorbent for the removal of dibenzothiophene, *J. Chem. Eng. Data* 57 (2012) 1713–1720.
- [15] C.J. Allender, C. Richardson, B. Woodhouse, C.M. Heard, K.R. Brain, Pharmaceutical applications for molecularly imprinted polymers, *Int. J. Pharm.* 195 (2000) 39–43.
- [16] D.S. Wang, X.X. Zhang, S.Q. Nie, W.F. Zhao, Y. Lu, S.D. Sun, C.S. Zhao, Photoresponsive surface molecularly imprinted poly (ether sulfone) microfibers, *Langmuir* 28 (2012) 13284–13293.
- [17] T. Kobayashi, P.S. Reddy, M. Ohta, M. Abe, N. Fujii, Molecularly imprinted polysulfone membranes having acceptor sites for donor dibenzofuran as novel membrane adsorbents: Charge transfer interaction as recognition origin, *Chem. Mater.* 14 (2002) 2499–2505.
- [18] L.C. Xu, J.M. Pan, Q.F. Xia, F.F. Shi, J.D. Dai, X. Wei, Y.S. Yan, Composites of silica and molecularly imprinted polymers for degradation of sulfadiazine, *J. Phys. Chem. C* 116 (2012) 25309–25318.
- [19] J.W. Zhang, Y.L. Liu, G.L. Wu, M. Schönhoff, X. Zhang, Bolaform supramolecular amphiphiles as a novel concept for the buildup of surface-imprinted films, *Langmuir* 27 (2011) 10370–10375.
- [20] J.M. Pan, H. Yao, L.C. Xu, H.X. Ou, P.W. Huo, X.X. Li, Y.S. Yan, Selective recognition of 2,4,6-trichlorophenol by molecularly imprinted polymers based on magnetic halloysite nanotubes composites, *J. Phys. Chem. C* 115 (2011) 5440–5449.
- [21] W.H. Zhou, C.H. Lu, X.C. Guo, F.R. Chen, H.H. Yang, X.R. Wang, Mussel-inspired molecularly imprinted polymer coating superparamagnetic nanoparticles for protein recognition, *J. Mater. Chem.* 20 (2010) 880–883.
- [22] R.Z. Ouyang, J.P. Lei, H.X. Ju, Artificial receptor-functionalized nanoshell: Facile preparation, fast separation and specific protein recognition, *Nanotechnology* 21 (2010) 185502–185510.
- [23] X. Chen, Z.H. Zhang, X. Yang, J.X. Li, Y.N. Liu, H.J. Chen, W. Rao, S.Z. Yao, Molecularly imprinted polymers based on multi-walled carbon nanotubes for selective solid-phase extraction of oleanolic acid from the roots of kiwi fruit samples, *Talanta* 99 (2012) 959–965.
- [24] D. Hirsemann, T.K.J. Köster, J. Wack, L. van Wüllen, J. Breu, J. Senker, Covalent grafting to  $\mu$ -hydroxycapped surfaces? A kaolinite case study, *Chem. Mater.* 23 (2011) 3152–3158.
- [25] L. Alagha, S.Q. Wang, L.J. Yan, Z.H. Xu, J. Masliyeh, Probing adsorption of polyacrylamide-based polymers on anisotropic basal planes of kaolinite using quartz crystal microbalance, *Langmuir* 29 (2013) 3989–3998.
- [26] Y. Turhan, M. Doğan, M. Alkan, Poly(vinyl chloride)/kaolinite nanocomposites: Characterization and thermal and optical properties, *Ind. Eng. Chem. Res.* 49 (2010) 1503–1513.

- [27] M.H. Karaoğlu, M. Doğan, M. Alkan, Removal of reactive blue 221 by kaolinite from aqueous solutions, *Ind. Eng. Chem. Res.* 49 (2010) 1534–1540.
- [28] H. Ming, K.M. Spark, R. Smart, Comparison of radio-frequency-plasma- and ion-beam-induced surface modification of kaolinite, *J. Phys. Chem. B* 105 (2001) 3196–3203.
- [29] Y. Komori, H. Enoto, R. Takenawa, S. Hayashi, Y. Sugahara, K. Kuroda, Modification of the interlayer surface of kaolinite with methoxy groups, *Langmuir* 16 (2000) 5506–5508.
- [30] P. Qu, J.P. Lei, L. Zhang, R.Z. Ouyang, H.X. Ju, Molecularly imprinted magnetic nanoparticles as tunable stationary phase located in microfluidic channel for enantioseparation, *J. Chromatogr. A* 1217 (2010) 6115–6121.
- [31] X.M. Jiang, W. Tian, C.D. Zhao, H.X. Zhang, M.C. Liu, A novel sol-gel-material prepared by a surface imprinting technique for the selective solid-phase extraction of bisphenol A, *Talanta* 72 (2007) 119–125.
- [32] L.G. Chen, X.P. Zhang, L. Sun, Fast and selective extraction of sulfonamides from honey based on magnetic molecularly imprinted polymer, *J. Agric. Food Chem.* 57 (2009) 10073–10080.
- [33] B.K. Nandi, A. Goswami, M.K. Purkait, Adsorption characteristics of brilliant green dye on kaolin, *J. Hazard. Mater.* 161 (2009) 387–395.
- [34] L.H. Liu, Y. Lin, Y.Y. Liu, H. Zhu, Q. He, Removal of methylene blue from aqueous solutions by sewage sludge based granular activated carbon: Adsorption equilibrium, kinetics, and thermodynamics, *J. Chem. Eng. Data* 58 (2013) 2248–2253.
- [35] P. Sharma, M.R. Das, Removal of a cationic dye from aqueous solution using graphene oxide nanosheets: Investigation of adsorption parameters, *J. Chem. Eng. Data* 58 (2013) 151–158.
- [36] M.Y. Xu, P. Yin, X.G. Liu, X.Q. Dong, Q. Xu, R.J. Qu, Preparation, characterization, adsorption equilibrium, and kinetics for gold-ion adsorption of spent buckwheat hulls modified by organodiphosphonic acid, *Ind. Eng. Chem. Res.* 52 (2013) 8114–8124.
- [37] J.M. Pan, H. Hang, X.X. Li, W.J. Zhu, M.J. Meng, X.H. Dai, J.D. Dai, Y.S. Yan, Fabrication and evaluation of temperature responsive molecularly imprinted sorbents based on surface of yeast via surface-initiated AGET ATRP, *Appl. Surf. Sci.* 287 (2013) 211–217.
- [38] Y. Li, X. Li, C.K. Dong, Selective recognition and removal of chlorophenols from aqueous solution using molecularly imprinted polymer prepared by reversible addition-fragmentation chain transfer polymerization, *Biosens. Bioelectron.* 25 (2009) 306–312.